Zhx2 (zinc fingers and homeoboxes 2) regulates major urinary protein gene expression in the mouse liver

Received for publication, November 16, 2016, and in revised form, February 19, 2017 Published, Papers in Press, March 3, 2017, DOI 10.1074/jbc.M116.768275

Jieyun Jiang[‡1], **Kate Townsend Creasy**[§2], **Justin Purnell**[‡], **Martha L. Peterson**[‡¶], **and Brett T. Spear**[‡§¶3]

From the[‡]*Department of Microbiology, Immunology, and Molecular Genetics,* [§]*Department of Pharmacology and Nutritional Sciences, and* [¶]*Markey Cancer Center, University of Kentucky College of Medicine, Lexington, Kentucky 40536*

Edited by Eric R. Fearon

The mouse major urinary proteins (Mups) are encoded by a large family of highly related genes clustered on chromosome 4. Mups, synthesized primarily and abundantly in the liver and secreted through the kidneys, exhibit male-biased expression. Mups bind a variety of volatile ligands; these ligands, and Mup proteins themselves, influence numerous behavioral traits. Although urinary Mup protein levels vary between inbred mouse strains, this difference is most pronounced in BALB/cJ mice, which have dramatically low urinary Mup levels; this BALB/cJ trait had been mapped to a locus on chromosome 15. We previously identified Zhx2 (zinc fingers and homeoboxes 2) as a regulator of numerous liver-enriched genes. *Zhx2* is located on chromosome 15, and a natural hypomorphic mutation in the BALB/cJ *Zhx2* allele dramatically reduces Zhx2 expression. Based on these data, we hypothesized that reduced Zhx2 levels are responsible for lower Mup expression in BALB/cJ mice. Using both transgenic and knock-out mice along with *in vitro* assays, our data show that Zhx2 binds Mup promoters and is required for high levels of Mup expression in the adult liver. In contrast to previously identified Zhx2 targets that appear to be repressed by Zhx2, Mup genes are positively regulated by Zhx2. These data identify Zhx2 as a novel regulator of Mup expression and indicate that Zhx2 activates as well as represses expression of target genes.

Mups[4] are 18- to 19-kDa proteins of the lipocalin superfamily that, as their name implies, are secreted in the urine at high concentrations (1, 2). As with other lipocalin proteins, Mups have the ability to bind small organic molecules such as pheromones. Although these small molecules have the ability to influence sexual and social behavior, including male aggression, Mup proteins themselves can also influence behaviors in rodents (3–6).

In mice, Mups are encoded by a multigene family comprised of 21 genes and 21 pseudogenes that are tightly clustered on chromosome 4 (7–9). *Mup* genes can be separated into two classes: six class A *Mup* genes that are 84–92% identical to each other at the DNA level and 15 highly related class B *Mup* genes that exhibit >97% identity (9). *Mup* genes are transcribed abundantly in the liver and at somewhat lower levels in secretory tissues, including the salivary, lachrymal, and mammary glands (10). They are also transcribed at higher levels in males and, as with other genes that exhibit this sex-biased expression, are influenced by testosterone, growth hormone and thyroxine (1, 11, 12). Although *Mup* genes are among the most highly expressed genes in the mouse liver, the factors that regulate Mup transcription are not known.

The *zinc fingers and homeoboxes 2* (*Zhx2*) gene belongs to a small gene family found only in vertebrates that also includes *Zhx1* and *Zhx3* (13–15). All three Zhx genes have the same unique structure, with the entire coding region on an unusually large third exon (16). The proteins encoded by these genes are predicted to contain two C_2-H_2 zinc fingers and four (or five) homeodomains; these domains suggest that Zhx proteins are involved in DNA binding (16). The initial phenotype associated with the mouse *Zhx2* gene was a mouse strain-specific difference in adult liver α-fetoprotein (AFP) levels. The AFP gene is expressed abundantly in the fetal liver, normally silenced at birth, and remains off in the adult liver but can be reactivated during liver regeneration and in hepatocellular carcinoma (HCC) (17, 18). A unique feature of AFP expression is seen in BALB/cJ mice, in which adult liver AFP mRNA levels are roughly 10- to 20-fold higher than what is seen in other strains, including other highly related BALB/c substrains (18, 19). This persistent AFP expression in BALB/cJ mice is due to a hypomorphic mutation in the BALB/cJ *Zhx2* gene (20, 21), which is located on chromosome 15 (22, 23). This mutation in BALB/cJ mice is due to the insertion of a mouse endogenous retroviral element into Zhx2 intron 1 that dramatically reduces Zhx2 mRNA levels (20, 21). Several other developmentally silenced genes, including *H19*, *Glypican 3* (*Gpc3*), and *Lipoprotein lipase*, are also targets of Zhx2 based on their elevated expression in the adult liver of BALB/cJ mice compared with other

This work is supported by Public Health Service Grants R01DK074816 (to B. T. S.), P20RR021954 (to B. T. S.), and T32DK007778 (to K. T. C.) and National Science Foundation Grant MCB-1158234 (to M. L. P.). The authors declare that they have no conflicts of interest with the contents of this article.

This article contains supplemental Experimental Procedures, Figs. S1 and S2, and Tables S1 and S2.

[1] To whom correspondence may be addressed: Dept. of Microbiology, Immunology, and Molecular Genetics, University of Kentucky College of Medicine, 800 Rose St., Lexington, KY 40536; Tel.: 859-323-5089; E-mail: jieyun.jiang2@uky.edu.

[2] Present address: University of California, Cardiovascular Research Institute, 555 Mission Bay Blvd. S., Rm. 282T, San Francisco, CA 94158.

[3] To whom correspondence may be addressed: Dept. of Microbiology, Immunology, and Molecular Genetics, University of Kentucky College of Medicine, 800 Rose St., Lexington, KY 40536; Tel.: 859-257-5167; E-mail: bspear@uky.edu.

[4] The abbreviations used are: Mup, major urinary protein; AFP, α-fetoprotein; HCC, hepatocellular carcinoma; TTR, transthyretin; E.V., empty vector; RT-qPCR, quantitative real-time RT-PCR; UAS, upstream activating sequence.

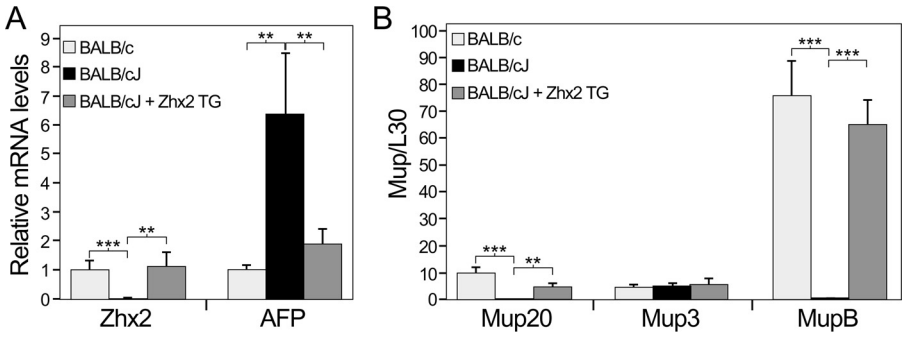

Figure 1. Low Mup expression in BALB/cJ liver is corrected in hepatocyte-specific Zhx2 transgenic mice. Livers were removed from age-matched adult male mice (4–6 mice/group). Total RNA was prepared, and mRNA levels were analyzed by RT-qPCR using primers described in supplemental Table 2. Zhx2, AFP, and Mup transcript levels were normalized against ribosomal L30 protein mRNA. *A*, hepatic Zhx2 levels are dramatically reduced in BALB/cJ mice compared with BALB/c mice ($Zhx2^{+}$) and restored to wild-type levels in BALB/cJ mice expressing a hepatocyte-specific TTR-Zhx2 transgene (*BALB/cJ + Zhx2 TG*). AFP is derepressed in BALB/cJ mice but restored to near wild-type levels in TTR-Zhx2 transgenic mice. Zhx2 and AFP levels in BALB/c mice were set at 1. *B*, the mRNA levels for Mup20 and class B Mups (using a primer pair that detects all three liver-expressed class B Mups) are dramatically reduced in BALB/cJ mice but found at similar levels in BALB/c and Zhx2 TG^{+} mice. Mup3 mRNA levels are not affected by changes in Zhx2 expression. Data are presented as mean ± S.D. **, $p < 0.01$; ***, $p < 0.001$.

strains (24–26). These *in vivo* data, as well as *in vitro* studies, indicate that Zhx2 represses target gene expression in the adult liver (23, 27, 28).

Variation in Mup protein levels is observed in different strains of mice (29). This difference is most pronounced in BALB/cJ mice, which express Mups at considerably lower levels than what is seen in other strains, including other BALB/c substrains (30). This reduced Mup expression in BALB/cJ mice was mapped to a locus on mouse chromosome 15 (30). The dramatic reduction in urinary Mup levels in BALB/cJ mice led us to investigate whether this trait was due to the Zhx2 mutation. Using BALB/c substrains, transgenic models, and recently developed Zhx2 knock-out mice, our data indicate that a number of *Mup* genes in the liver are targets of Zhx2 regulation. However, in contrast to previous Zhx2 targets, which are elevated when Zhx2 levels are reduced, Mup expression decreases when Zhx2 levels are lower. Using transient transfections and ChIP, we show that Zhx2 directly binds and activates Mup promoters and that this activation is governed primarily through the Zhx2 homeodomain region. These data provide further insight into Mup expression during liver development and expand our understanding of Zhx2 regulation of target genes in the adult liver.

Results

Reduced hepatic Mup gene expression in BALB/cJ mice is due to the Zhx2 mutation

Urinary Mup levels in BALB/cJ male mice are dramatically lower than in other mouse strains (30). Another trait unique to the BALB/cJ substrain is elevated AFP expression in the adult liver, which, as we showed previously, is due to a hypomorphic mutation in the BALB/cJ *Zhx2* gene (20). To test whether the BALB/cJ Zhx2 mutation is responsible for reduced Mup protein levels, the expression of several *Mup* genes was analyzed by RT-qPCR in the adult male liver of the BALB/c substrain, which have a wild-type *Zhx2* gene, and the BALB/cJ substrain. Studies were performed in male mice because Mups are synthesized at much higher levels in male than in female mice. Of the 21 *Mup* genes, we focused our analysis on the class A *Mup20* and *Mup3* and class B *Mup7*, *Mup10*, and *Mup19* genes (using Mouse Genome Informatics nomenclature) because these exhibit the highest expression in the liver (9). Zhx2 mRNA levels in BALB/cJ mice were roughly 4% of that seen in BALB/c mice, and, as expected, AFP mRNA levels were over 6-fold higher (Fig. 1*A*). Mup20 mRNA levels were dramatically lower in BALB/cJ, being only ~1% of the level in age-matched adult BALB/c liver. In contrast to *Mup20*, expression of the class A *Mup3* gene was not affected by the Zhx2 mutation. Expression of the highly related class B *Mup* genes in BALB/cJ was reduced to 0.3% of the levels seen in BALB/c mice (Fig. 1*B*).

To confirm that reduced Mup expression in BALB/cJ mice was due to the Zhx2 mutation, we analyzed Mup expression in *TTR-Zhx2* transgenic BALB/cJ mice, which express Zhx2 specifically in hepatocytes. Hepatic Zhx2 and AFP mRNA levels in these transgenic mice are found at roughly the same levels as seen in BALB/c mice, consistent with previous studies (Fig. 1*A*) (20). The presence of the *TTR-Zhx2* transgene in BALB/cJ mice restored Mup20 and class B Mup expression to levels that were roughly 45% and 86% of that seen in BALB/c mice, respectively, whereas Mup3 mRNA levels were not substantially affected by the *TTR-Zhx2* transgene (Fig. 1*B*). Because Mups are synthesized primarily in the liver, these data indicate that the low urinary Mup levels seen previously in BALB/cJ mice are due to reduced hepatic Mup20 and class B Mup mRNA levels. The dramatic reduction in Mup expression in BALB/cJ mice and restoration of near wild-type Mup mRNA levels in *TTR-Zhx2* BALB/cJ mice demonstrate that Zhx2 is required for normal Mup expression in the adult liver. In contrast to previously identified Zhx2 targets that are negatively regulated by Zhx2, Mup20 and class B Mup mRNA levels are positively regulated by Zhx2.

Mup expression is reduced in Zhx2 knock-out mice

Our studies in BALB/c substrains indicated that Zhx2 is required for normal Mup expression in the adult liver. Studies were also performed in Zhx2 knock-out mice in which the entire Zhx2 protein-coding region in exon 3 is flanked by l*oxP* sites; Cre-mediated excision therefore removes the entire Zhx2 reading frame (31). These mice were bred to *E2a-Cre* and *Alb-Cre* transgenic mice to obtain whole-body ($Zhx2^{KO}$) and hepa-

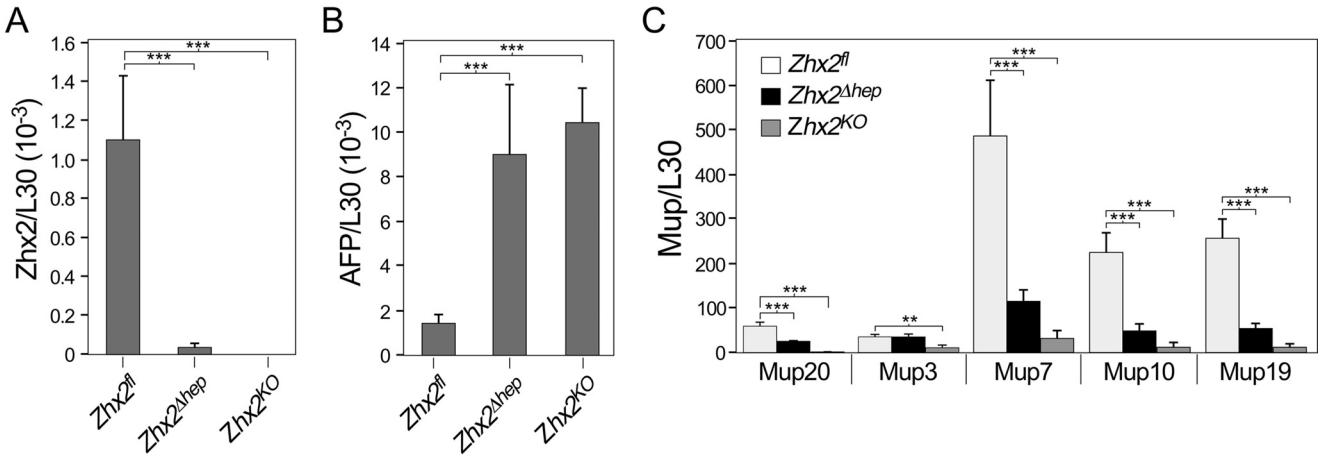

Figure 2. Hepatic Mup mRNA levels are reduced in Zhx2 knock-out mice compared with *Zhx2*^{fl} mice. Livers were removed from age-matched adult male mice (4–6 mice/group). Total RNA was prepared, and mRNA levels were analyzed by RT-qPCR using primers shown in supplemental Table 2. Zhx2, AFP, and Mup transcript levels were normalized against ribosomal L30 protein mRNA. *A*, hepatic Zhx2 levels are dramatically reduced in *Zhx2*$^{\Delta hep}$ mice and not detectable in *Zhx2*^{KO} mice. *B*, AFP mRNA levels are increased similarly in the livers of both *Zhx2*$^{\Delta hep}$ mice and *Zhx2*^{KO} mice. *C*, Mup20 and class B Mup (Mup7, Mup10, and Mup 19) mRNA levels are reduced to a greater extent in *Zhx2*^{KO} mice than in *Zhx2*$^{\Delta hep}$ mice, whereas a reduction in Mup3 levels is only seen in *Zhx2*^{KO} mice. Data are presented as mean ± S.D. **, $p < 0.01$; ***, $p < 0.001$.

tocyte-specific (*Zhx2*$^{\Delta hep}$) Zhx2 deletion, respectively. Zhx2 mRNA levels in *Zhx2*$^{\Delta hep}$ mice were 3% the levels found in *Zhx2*^{fl} mice controls and were undetectable in *Zhx2*^{KO} mice (Fig. 2*A*). We showed previously by immunofluorescence staining that the higher Zhx2 levels in *Zhx2*$^{\Delta hep}$ mice compared with *Zhx2*^{KO} mice is due to Zhx2 expression in non-parenchymal cells (31). This was confirmed by RT-qPCR analysis in purified parenchymal and non-parenchymal cells (supplemental Fig. 1). As expected, AFP levels increased 6- to 7-fold in *Zhx2*$^{\Delta hep}$ and *Zhx2*^{KO} mice compared with age-matched *Zhx2*^{fl} controls (Fig. 2*B*). Mup expression was decreased in the knock-out mice similarly to what was observed in BALB/cJ mice. Mup20 levels were reduced to 41% and 2% in *Zhx2*$^{\Delta hep}$ and *Zhx2*^{KO} mice, respectively, compared with *Zhx2*^{fl} controls. A similar reduction was seen with class B *Mup* genes. Using gene-specific primers for the hepatic class B Mups, we found that Mup 7, Mup 10, and Mup 19 levels were reduced to 23%, 23%, and 21%, respectively, in Zhx2$^{\Delta hep}$ livers, and all were reduced to 6% in *Zhx2*^{KO} livers compared with *Zhx2*^{fl} controls. In contrast, Mup3 expression was affected to a lesser extent in that no significant change was seen in *Zhx2*$^{\Delta hep}$ mice whereas Mup3 expression in *Zhx2*^{KO} mice was 34% of levels in *Zhx2*^{fl} controls (Fig. 2*C*). To test whether Mup protein levels correlated with reduced hepatic Mup mRNA, Mup proteins in the liver were analyzed. Western-blotting analysis with a pan-Mup antiserum indicated that Mup protein levels were reduced in both *Zhx2*$^{\Delta hep}$ and *Zhx2*^{KO} adult male livers, although the reduction was most dramatic in *Zhx2*^{KO} livers (Fig. 3*A*). A similar pattern was seen when Western-blotting analysis was performed with urine samples (Fig. 3*B*). In contrast to liver, the anti-Mup antibodies recognized two Mup isoforms in urine; the abundant, slower-migrating band had the same molecular weight as the band seen in the liver and was most responsive to changes in Zhx2. Based on previous studies, the low-abundance, faster-migrating band is likely encoded by the atypical Mup17 gene (29). Coomassie staining of whole urine (Mups account for a vast majority of urinary proteins in healthy male mice (32)) demonstrated that the predominant urinary Mup isoform is reduced in both hepatocyte-specific and whole-body knock-out mice, with a greater reduction seen in *Zhx2*^{KO} urine (Fig. 3*C*). The slower-migrating protein (Fig. 3*C*, *asterisk*) found in the urine did not react with the Mup antiserum but served as a control for uniform loading.

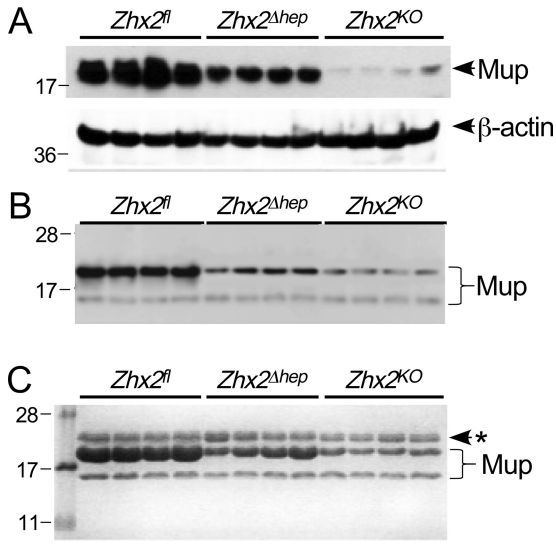

Figure 3. Zhx2 positively regulates Mup protein levels. Livers and urine were obtained from age-matched adult male mice that were homozygous for the *Zhx2*^{fl}, *Zhx2*$^{\Delta hep}$, or *Zhx2*^{KO} alleles (4 mice/group, each lane represents a single mouse). *A* and *B*, liver cell lysates (*A*) and urine (*B*) were analyzed by Western blotting using a pan-Mup antiserum. Hepatic Mup protein levels are moderately reduced in *Zhx2*$^{\Delta hep}$ livers and dramatically reduced in *Zhx2*^{KO} livers. Blots were reprobed for β-actin to control for variations in protein loading. The predominant urinary Mup proteins showed a reduction in *Zhx2*$^{\Delta hep}$ and *Zhx2*^{KO} mice that was similar to that seen in liver. The faster-migrating, lower-abundance Mup protein (encoded by the divergent Mup17 gene) was found in urine and not responsive to changes in Zhx2 levels. *C*, total urine was collected and clarified, and urinary proteins were separated by 15% SDS-PAGE and stained with LabSafe Gel Blue. Levels of the predominant urinary Mup proteins were reduced in *Zhx2*$^{\Delta hep}$ mice and, to a greater extent, in *Zhx2*^{KO} mice. The slower-migrating band (*asterisk*) served as a loading control.

Mup expression is developmentally activated in the postnatal liver

Previously identified Zhx2 targets are expressed abundantly in the fetal liver and repressed within the first 4 weeks after

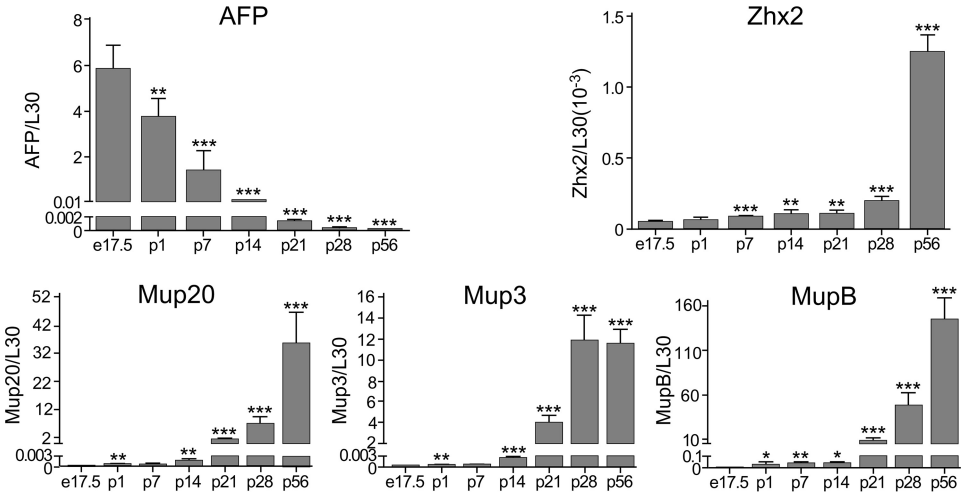

Figure 4. Mup genes are developmentally activated in the postnatal liver. Livers were removed from male mice at E17.5 and various postnatal time points up to 8 weeks (P1-P56). Total RNA was prepared and analyzed by RT-qPCR. Levels of Zhx2, AFP, and Mup transcripts were normalized against ribosomal L30 protein mRNA. AFP levels decreased ~10^5-fold during this period. Zhx2 mRNA levels increased gradually between E17.5 and P28 and then increased ~6.5-fold between P28 and P56. Mup mRNA levels also increased postnatally, with the most dramatic increase occurring between P14 and P21. Overall, the increase in expression of Mup genes was ~10^5-fold, which was roughly equivalent to the -fold decrease in AFP levels (supplemental Table 1). Data are presented as mean ± S.D. *, $p < 0.05$; **, $p < 0.01$; ***, $p < 0.001$ relative to E17.5.

birth. Because *Mup* genes appear to be positively regulated by Zhx2, we predicted that Mup expression would increase during postnatal liver development. Steady-state Mup20, Mup3, and class B Mup mRNAs are barely detectable at embryonic day 17.5 (E17.5) and remain at very low levels up to postnatal day 14 (P14; Fig. 4 and supplemental Table 1). Expression of all these Mups sharply increase at P21. By 8 weeks after birth, expression of all Mups analyzed had increased 10^5-fold over embryonic levels. During this same time, AFP mRNA levels decrease 10^5-fold, consistent with previous studies (18), whereas Zhx2 mRNA levels increase ~35-fold (Fig. 4 and supplemental Table 1). Interestingly, *Mup20* and the class B *Mup* genes exhibit a substantial increase between P28 and P56, the same period when Zhx2 shows the greatest increase.

Zhx2 activates Mup expression in vitro

The *in vivo* mouse data indicate that Zhx2 positively regulates Mup expression in the adult liver. We asked whether this regulation could be observed *in vitro*, which would provide a system to mechanistically explore how Zhx2 controls Mup expression. To determine whether Zhx2 can activate endogenous Mup genes, we transiently expressed a Zhx2-GFP fusion protein in the AML12 mouse hepatocyte cell line. After 48 h, cells were visualized by fluorescence, and total RNA was extracted. Fluorescence microscopy indicated that roughly 30–40% of transfected cells expressed Zhx2-GFP and that the fusion protein was localized to the nucleus (supplemental Fig. 2), as had been observed previously (14, 28). RT-qPCR shows that endogenous Mup20, Mup3 and class B Mup mRNA levels increase in Zhx2-GFP-transfected cells compared with control empty vector (pcDNA3.1 alone)-transfected cells (Fig. 5). In contrast, expression of Transthyretin (TTR), which is not affected by the loss of Zhx2 in BALB/cJ mice (24), does not change in Zhx2-GFP-transfected AML12 cells (Fig. 5).

To determine whether Zhx2 activated expression through the Mup promoter region, a 1.4-kb region containing the

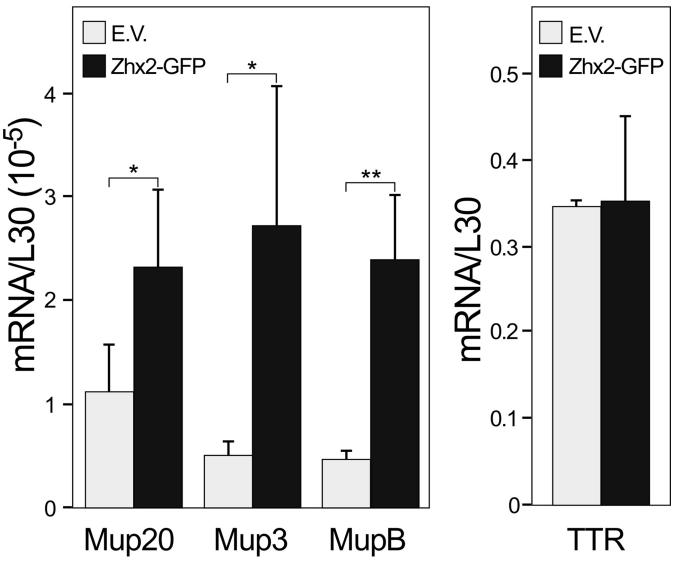

Figure 5. Endogenous Mup expression is increased in Zhx2-GFP-transfected AML12 cells. The mouse hepatocyte AML12 cell line was transfected with the pcDNA3.1 E.V. control or pcDNA3.1 encoding a Zhx2-GFP fusion protein (Zhx2-GFP) and analyzed after 48 h. Levels of endogenous transcripts in transfected cells were analyzed by RT-qPCR. Mup20, Mup3, and class B Mups were activated by Zhx2. Expression of TTR was not affected by increased Zhx2 expression. Data are presented as mean ± S.D. *, $p < 0.05$; **, $p < 0.01$.

Mup20 promoter (−1373 to +32) was inserted into the pGL4.14[*luc2*/Hygro] luciferase reporter gene to generate Mup20^{p}-luc. Plasmids encoding Zhx2 and Mup20^{p}-luc were co-transfected into AML12 cells and HepG2 human hepatoma cells along with a *Renilla* luciferase vector to control for variations in transfection efficiency. The control pGL4.14 plasmid was not affected by Zhx2. However, co-transfected Zhx2 increased luciferase levels 2.3-fold and 1.5-fold from Mup20^{p}-luc in HepG2 and AML12 cells, respectively (Fig. 6*A*). To further investigate the region(s) of the Mup20 promoter responsive to Zhx2, a series of promoter deletion constructs were inserted into pGL4.14 and co-transfected with Zhx2 in HepG2

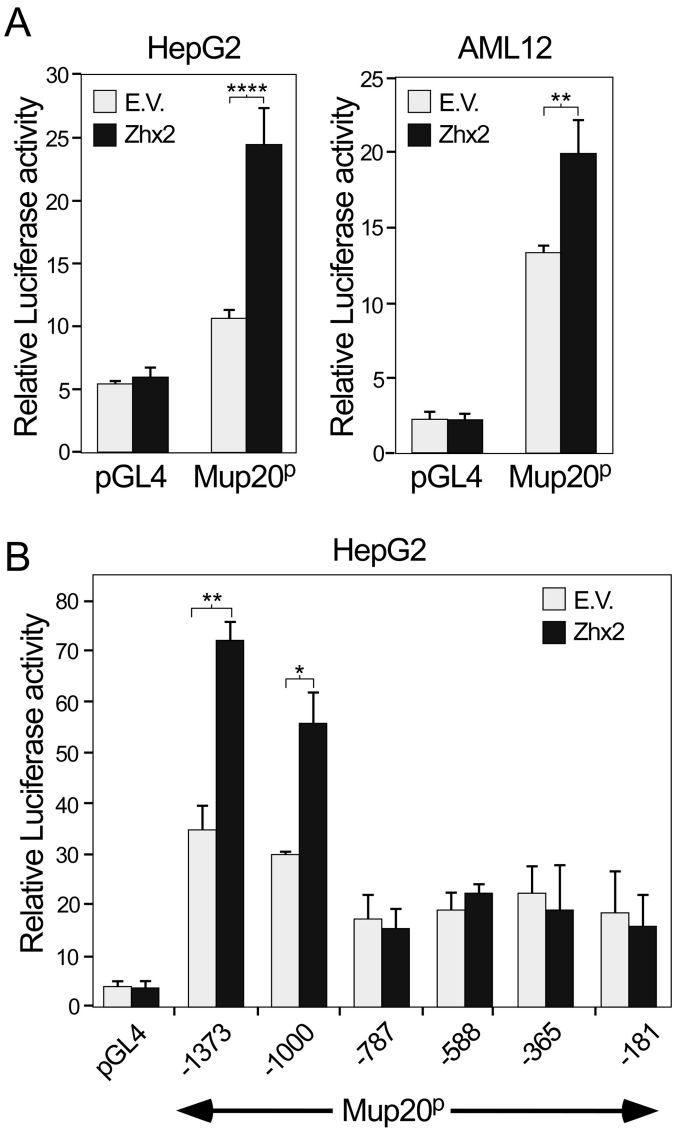

Figure 6. A region of the Mup20 promoter between −787 and −1000 is responsive to Zhx2. *A*, HepG2 cells and AML12 cells were transfected with pGL4 control or Mup20^{p}-Luc reporter genes along with pcDNA3.1 E.V. or the Zhx2 expression vector; *Renilla* luciferase was also included to control for variations in transfection efficiency. After 48 h, cells were harvested, and lysates were analyzed for firefly/*Renilla* luciferase. pGL4 was not responsive to Zhx2, whereas the Mup20 promoter was activated by Zhx2 in both HepG2 and AML12 cells. *B*, a series of Mup20 promoter deletion constructs were transfected with E.V. or Zhx2 in HepG2 cells and analyzed as described in *A*. Mup20 promoter fragments extending to −1373 and −1000 were responsive to co-transfected Zhx2, whereas fragments extending to −787, −588, −365, and −181 were no longer responsive. Data are presented as mean ± S.D. *, $p < 0.05$; **, $p < 0.01$; ***, $p < 0.001$.

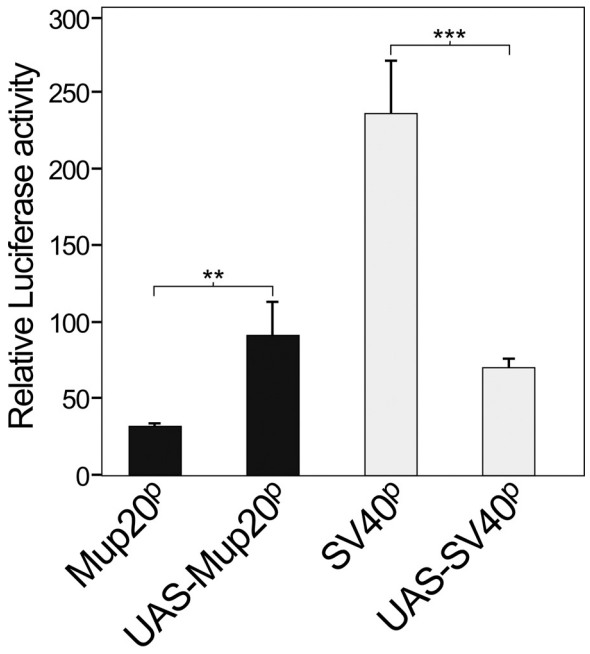

Figure 7. Gal4DBD-Zhx2 activates the Mup20 promoter and represses the SV40 promoter when tethered by UAS motifs. HEK293 cells were co-transfected with Gal4DBD-Zhx2 along with luciferase expression vectors containing the Mup20 promoter (*Mup20^{p}*), Mup20p and 5× UAS copies (*UAS-Mup20^{p}*), SV40 promoter (*SV40^{p}*), or SV40p and 5× UAS copies (*UAS-SV40^{p}*). After 48 h, cells were harvested, and lysates were analyzed for firefly/*Renilla* luciferase. The presence of the UAS increased Gal4DBD-Zhx2 responsiveness of Mup20p nearly 3-fold and repressed SV40p roughly 3.4-fold. Data are presented as mean ± S.D. **, $p < 0.01$; ***, $p < 0.001$.

cells. Promoter fragments extending ~1.4 and 1.0 kb upstream of Mup20 exon 1 were activated by Zhx2, whereas further deletions resulted in non-responsiveness to Zhx2 (Fig. 6*B*). This indicates that the Zhx2-responsive element of the Mup20 promoter region resides between −1000 and −787.

Zhx2 activates the Mup20 promoter through the homeodomain region

Zhx2 is generally considered to be a transcriptional repressor. However, our transfection data indicate that Zhx2 can activate the Mup20 promoter. This positive regulation of Mup genes is consistent with our mouse studies showing decreased Mup levels when Zhx2 is reduced. To further explore this regulation, the Gal4 DNA binding domain was fused to the entire Zhx2 coding region to generate Gal4DBD-Zhx2; the Gal4DBD will tether Zhx2 to Gal4 binding sites (UAS). This fusion protein was co-transfected into HEK293 cells with Mup20^{p}-luc or Mup20^{p}-luc fused to 5 tandem Gal4 binding sites (UAS). As controls, luciferase expression vectors containing the SV40 promoter, with or without the UAS, were also co-transfected with Gal4DBD-Zhx2. The presence of the UAS increased the responsiveness of the Mup20 promoter to Gal4DBD-Zhx2 nearly 3-fold, consistent with Mup20 promoter activation by Zhx2 (Fig. 7). In contrast, the presence of the UAS led to a ~3.4-fold repression of the SV40 promoter by Gal4DBD-Zhx2 (Fig. 7).

Zhx proteins, including Zhx2, contain two amino-terminal zinc finger motifs and multiple (4–5) predicted C-terminal homeodomains. To begin to localize the Zhx2 region responsible for Mup activation, we created hybrid proteins in which the zinc finger and homeodomain regions of Zhx1 and Zhx2 were swapped (Fig. 8*A*). These hybrid proteins, as well as Zhx2 and Zhx1, were co-transfected with Mup20^{p}-luc into HEK293 cells (Fig. 8). As seen previously, Zhx2 activates Mup20^{p}-luc roughly 2.3-fold. In contrast, Zhx1 did not activate Mup20^{p}-luc. The hybrid Zhx protein containing Zhx2 homeodomains significantly activated Mup20^{p}-luc, indicating that this region, rather than the zinc-finger region, is primarily responsible for activating the Mup20 promoter (Fig. 8).

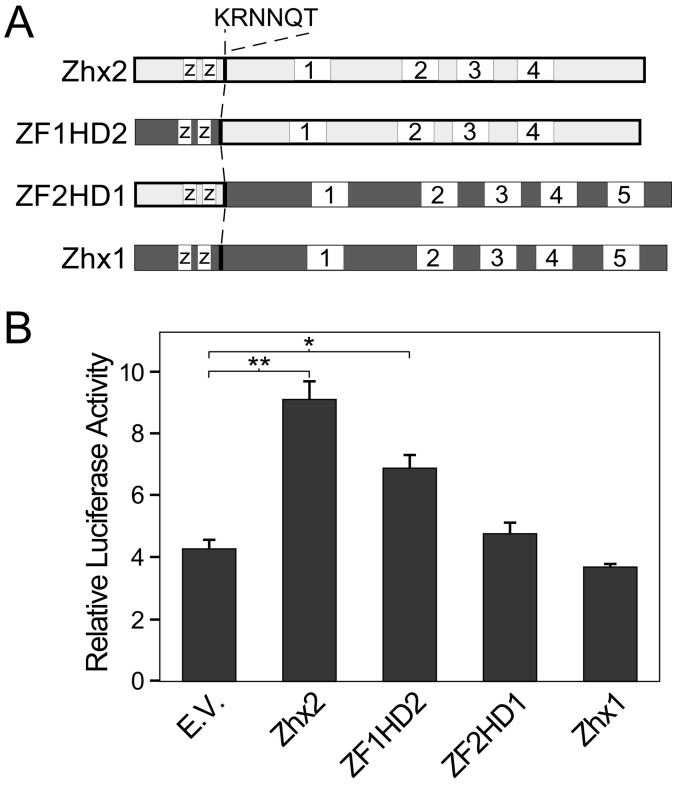

Figure 8. The homeodomain region of Zhx2 is primarily responsible for activation of the Mup20 promoter. *A*, diagram showing Zhx2 and Zhx1 with zinc fingers (*z*) and homeodomains (*1–5*) are shown. Hybrid proteins in which the zinc finger region of Zhx1 is fused to the homeodomain region of Zhx2 (*ZF1HD2*) or the zinc finger region of Zhx2 is fused to the homeodomain region of Zhx1 (*ZF2HD1*) were generated at a conserved KRNNQTV site just downstream of the zinc finger domain region. *B*, HEK293 cells were co-transfected with Mup20^{P}-Luc and Zhx expression vectors or pcDNA3.1 E.V. *Renilla* luciferase was also included to control for variations in transfection efficiency. After 48 h, cells were harvested, and lysates were analyzed for firefly/*Renilla* luciferase. Zhx2 and ZF1HD2, but not ZF2HD1 or Zhx1, significantly activated Mup20^{P}-Luc. Data are presented as mean ± S.D. *, $p < 0.05$; **, $p < 0.01$.

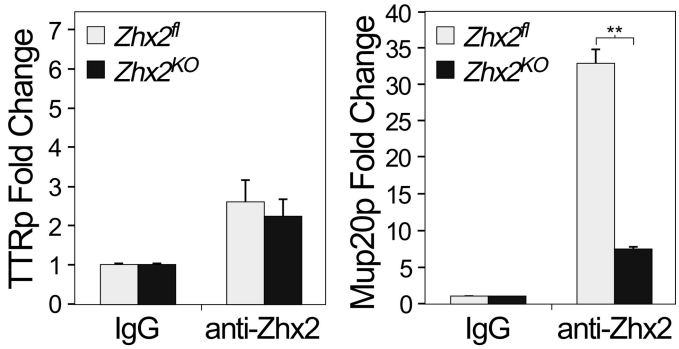

Figure 9. Zhx2 binds the Mup20 promoter *in vivo*. ChIP was performed using control IgG and anti-Zhx2 antibodies with livers from adult male *Zhx2^{fl}* and *Zhx2^{KO}* mice. For both genes, levels of IgG in *Zhx2^{fl}* mice were set to 1. The data indicate that Zhx2 binds the Mup20 promoter. Although the anti-Zhx2 shows somewhat increased binding to the TTR promoter compared with the IgG control, there is no difference between the *Zhx2^{fl}* and *Zhx2^{KO}* samples. Data presented as mean ± S.D. **, $p < 0.01$.

Zhx2 binds directly to the Mup20 and class B Mup promoters in vivo

To determine whether Zhx2 directly binds Mup promoters *in vivo*, ChIP was performed using livers from *Zhx2^{fl}* and *Zhx2^{KO}* adult male mice. We focused on Mup20 because our transfections localized Zhx2 binding to a region between −1000 and −787 (Fig. 6*B*). The TTR promoter was used as a control because the *TTR* gene is not a Zhx2 target. Although the Zhx2 ChIP signal for the TTR promoter was ~2-fold higher than the IgG controls, this binding was the same in *Zhx2^{fl}* and *Zhx2^{KO}* liver and thus considered background (Fig. 9). However, using primers that span the −884 to −759 region of the Mup20 promoter, an ~4.4-fold enrichment of Zhx2 binding to the Mup20 promoter was observed in *Zhx2^{fl}* liver compared with the *Zhx2^{KO}* liver (Fig. 9). A similar pattern was observed using primers for the class B Mup promoters (the primers will amplify Mup7, Mup10, and Mup19 promoters; data not shown). These data indicate that Zhx2 can directly bind Mup promoters *in vivo*.

Discussion

The *Mup* multigene family is ideal to study aspects of mammalian gene regulation, including coordinated control of multiple related genes, sex-biased expression, and tissue-specific expression. Most mammalian species have a single *Mup* gene (humans have only a single non-functional Mup pseudogene), whereas mice and rats have 21/21 and 9/13 clustered *Mup* genes/pseudogenes, respectively (9). In mice, Mups are expressed primarily in males. Although different Mups are expressed in different tissues and at different levels, the liver is the primary site of Mup synthesis. In fact, *Mups* are among the most highly expressed genes in the adult male mouse liver, with ~5% of the total mRNA being transcribed from this gene family (11). However, the basis for Mup expression in the liver or other organs is poorly understood. Here we show that Zhx2 is required for robust Mup expression in the adult male liver, although the liver-enriched *Mup* genes (*Mup20*, *Mup3*, and the class B *Mup7*, *Mup10*, and *Mup19*) exhibit differential responsiveness to Zhx2. Mup20 mRNA levels in BALB/cJ and *Zhx2^{KO}* mice are 1–2% the levels of age-matched wild-type controls. A similar pattern is seen with hepatic class B Mups; mRNA levels are less than 4% in BALB/cJ and *Zhx2^{KO}* mice compared with control mice. Mup3 expression appears to be less responsive to changes in Zhx2; no difference in hepatic Mup3 mRNA levels were seen in BALB/cJ and BALB/c livers, whereas a modest reduction was seen in *Zhx2^{KO}* mice. Curiously, in contrast to the *in vivo* data, Mup3 is equally, if not more responsive, than Mup20 and class B Mups in Zhx2-transfected AML12 cells. One possible explanation for this differential response is that the chromatin (histone modification, DNA methylation) of Mup3 in the intact liver and AML12 cells is different. A second possibility is that Mup3 is expressed in non-parenchymal cells (*i.e.* non-hepatocytes) in the liver. Along these lines, all *Mup* genes examined were reduced to a greater extent in *Zhx2^{KO}* livers than in *Zhx2$^{\Delta hep}$* livers, suggesting that Mup genes might be expressed in non-parenchymal cells or that these cells influence Mup expression in hepatocytes. Although our analysis has focused on the liver, which is the major site of Mup synthesis, certain Mups are expressed in other mouse tissues, including the lachrymal, salivary, and mammary glands (10). Zhx2 is also ubiquitously expressed (20). The role of Zhx2 in controlling expression of Mups and other target genes in these glands and other non-hepatic tissues is ongoing.

The mechanism by which Zhx2 controls target gene expression is not fully understood. A consensus Zhx2 binding site has not been identified, and it is not known which of the genes that are dysregulated in the absence of Zhx2 are direct or indirect targets. However, Zhx2 binds to and represses the Cyclin A and Cyclin E promoters (28), whereas the transfection and ChIP data presented here show that Zhx2 binds directly to and activates Mup promoters. Deletion analysis indicates that a region of the Mup20 promoter between −1000 and −787 is the target of Zhx2 activation. Further analysis of this region should help identify a specific Zhx2 binding site. It will be interesting to determine whether this site is also found in other Zhx2 targets, including those that are repressed by Zhx2. Having found that the Zhx2 homeodomain region is responsible for Mup promoter activation, studies with hybrid proteins can further localize the activation domains within Zhx2.

The ability of Zhx2 to positively or negatively regulate target genes is of particular interest to us. The initial analysis of human ZHX2 utilized cell culture systems to analyze ZHX2 function (14). These studies included co-transfections with Zhx2-Gal4DBD fusion proteins and SV40 promoter-luciferase reporter constructs linked to UAS. These studies indicated that Zhx2-Gal4DBD, when tethered to the UAS, could repress the SV40 promoter (14). We repeated this experiment and obtained the same result (Fig. 7). However, using this same system, we found that the presence of the UAS increases Gal4DBD-Zhx2 responsiveness of the Mup20 promoter nearly 3-fold over Zhx2 alone (Fig. 7). These data indicate that Zhx2 activation or repression of target promoters is context-dependent, *i.e.* requires gene-specific interactions with other factors and/or chromatin remodeling complexes. Although other factors that directly control Mup genes have not been identified, expression of several Mups decreases dramatically in HNF4α knock-out mice and decrease to a lesser extent in Stat5b-deficient mice (33).

Interestingly, positively regulated *Mups* and genes that are negatively regulated by Zhx2 exhibit similar but opposite expression patterns under multiple conditions, including development, liver regeneration, and in HCC. For example, steady-state AFP mRNA levels in mouse liver decrease over 10^5-fold within the first 4 weeks after birth. In contrast, expression of hepatic Mups increases 10^4- to 10^5-fold during this same period. AFP and other negatively regulated Zhx2 targets are transiently activated in regenerating liver, whereas Mup expression is decreased during this period.[5] Because AFP and all other previously identified Zhx2 targets are often activated in HCC, we would predict that Mups would be repressed in liver tumors. This possibility is supported by an earlier mouse study (34). Our preliminary analysis also indicates that expression of some, but not all, Mups are lower in mouse HCC samples compared with normal adult liver.[5]

Our initial interest in Zhx2 regulation of *Mup* genes came from the observation that urinary Mup levels are dramatically reduced in BALB/cJ mice (30). Having shown a direct relationship between Zhx2 and Mup expression raises the possibility that Zhx2 might influence Mup-associated traits. Mups are known to influence a variety of behaviors in mice, including male-male aggression. Zhx2 is mutated in BALB/cJ but not in other BALB/c substrains.[6] BALB/cJ mice exhibit higher fighting behavior compared with the highly related BALB/cN substrain, and this trait is controlled by a single locus (35, 36). A genome-wide analysis of loci associated with male-male aggression was performed using F2 offspring of a BALB/cJ (high aggression) X A/J (low aggression) cross (37). This genetic study identified three loci that influence aggression, including one tightly associated with the *D15Mit46* microsatellite marker, which is also tightly linked to *Zhx2* (23). Future studies can determine whether Zhx2 influences behavior in mice and whether this influence is associated with altered Mup expression.

The identification of Zhx2 began with the observation that AFP (19) as well as other fetally expressed genes (24, 25) continue to be expressed in the postnatal BALB/cJ liver. Zhx2 also controls the expression of hepatic genes that govern lipid homeostasis, and altered Zhx2 expression leads to changes in serum lipid levels (26). In this regard, it is interesting that two human genome-wide association studies have identified SNPs in Zhx2 that associate with carotid intima media thickness, a subclinical measure of atherosclerotic lesions (38, 39). More recently, we have found that female-biased *Cyp* genes are repressed by Zhx2 in the male liver, demonstrating that Zhx2 contributes to sex-biased gene expression (31). However, many of these previously identified targets exhibit modest changes in expression in the absence of Zhx2. AFP levels are elevated ~10-fold in the absence of Zhx2 but still repressed about 10^4-fold compared with what is found in the fetal liver. Female-biased Cyps are expressed at higher levels in adult male Zhx2-deficient livers but still expressed at significantly lower levels than what is seen in adult female liver. In contrast, expression of Mup20 and the class B Mup genes in the adult liver is highly dependent on Zhx2. This strong association between Zhx2 and hepatic Mup expression suggests that Mups will provide a more robust system to explore the mechanism by which Zhx2 regulates target gene expression.

In summary, the data presented here provide further evidence that Zhx2 is an important regulator of gene expression in the adult liver, including developmental regulation, sex-biased expression, and changes in gene expression during liver disease, including HCC. Many of the genes that are dysregulated in the absence of Zhx2 are associated with metabolism. Although Mups are most frequently associated with behavior, there is evidence that Mups can regulate lipid and glucose metabolism in mice (40). Because Zhx2 is expressed ubiquitously, it is likely that it also regulates genes in other tissues.

Experimental procedures

Mice and treatments

All mice were housed in the University of Kentucky Division of Laboratory Animal Research facility in accordance with Institutional Animal Care and Use Committee-approved protocols. C3H/HeJ (C3H), BALB/cJ, and C57BL/6J (BL/6) mice

[5] J. Jiang and B. T. Spear, unpublished observations.

[6] M. Al-Kafajy and B. T. Spear, unpublished data.

were purchased from The Jackson Laboratory; BALB/c mice, which have a wild-type *Zhx2* allele, were obtained from Charles River. The *TTR-Zhx2* transgenic mice (on a BALB/cJ background) express Zhx2 from a hepatocyte-specific transthyretin promoter-enhancer cassette (41), were generated by the University of Kentucky Transgenic Mouse Facility, and were described previously (20). To generate Zhx2 knock-out mice, exon 3, which encodes the entire Zhx2 coding region, was flanked by two *loxP* sites to generated a Zhx2 floxed allele ($Zhx2^{fl}$) in C57BL/6 mice (31). The $Zhx2^{fl}$ mice were crossed with *Alb-Cre* mice (The Jackson Laboratory, 003574) to generate hepatocyte-specific Zhx2 knock-out mice ($Zhx2^{\Delta hep}$) or crossed with *E2a-Cre* mice (The Jackson Laboratory, 003724) to generate whole-body Zhx2 knock-out mice ($Zhx2^{KO}$). For developmental time point studies, female C3H mice were bred to male BL/6 mice (both strains have wild-type *Zhx2* alleles), and female mice were monitored for vaginal plugs to estimate the time of fertilization. For E17.5, pregnant females were killed by CO_2 asphyxiation at 17.5 days post-conception, and fetuses were removed. For postnatal time points, mice were killed by CO_2 asphyxiation at the designated times after birth. Purification of parenchymal hepatocytes and non-parenchymal cells is described in the supplemental Experimental Procedures.

Cloning of reporter genes and expression vectors

The Mup20 promoter region (−1373 to +32) was amplified from BL/6 mouse genomic DNA. The purified PCR product was cloned into the pGEM-T Easy vector (Promega) and confirmed by sequencing. This ~1.4-kb fragment was excised and recloned into the pGL4.14[*luc2*/Hygro] luciferase vector (Promega). The resulting plasmid was designated Mup20^{P}-luc. Additional 5′ primers were used to generate Mup20 promoter subfragments beginning at −1000, −787, −588, −365, and −181; all subfragments ended at +32. A 210-bp fragment containing the SV40 promoter was excised from pGL3-Luciferase and inserted into pGL4.14[*luc2*/Hygro] to generate SV40^{P}. The Zhx expression vectors were constructed in our laboratory using pcDNA3.1. Briefly, full-length Zhx2 and Zhx1 amplicons with a 5′ FLAG epitope were amplified from BL/6 mouse genomic DNA, cloned into pGEM-T Easy, sequenced, and recloned into pcDNA3.1 to generate FLAG-Zhx2 (Zhx2) and FLAG-Zhx1 (Zhx1), respectively. A full-length EGFP clone was inserted in-frame 3′ of Zhx2 to generate the FLAG-Zhx2-GFP plasmid (Zhx2-GFP). A fragment containing the 148-amino acid DNA-binding domain of Gal4 was inserted in-frame 5′ of Zhx2 to generate Gal4DBD-Zhx2. To generate UAS-Mup20^{P} and UAS-SV40^{P}, a fragment containing five copies of the optimized Gal4 DNA-binding motif (42) was inserted upstream of Mup20^{P} and SV40^{P} to generate UAS-Mup20^{P} and UAS-SV40^{P}, respectively. The Gibson Assembly Cloning Kit (New England Biolabs, E5510S) was used to generate Zhx1-Zhx2 hybrid proteins. The hybrid proteins were fused at a conserved KRNNQT sequence located between the zinc finger and homeodomain regions of Zhx1 and Zhx2. Cloning details are available upon request.

Cell lines and transient transfections

AML12, a mouse hepatocyte cell line, HepG2, a human hepatoma cell line, and HEK293, a human embryonic kidney cell line, were obtained from the ATCC (Manassas, VA). AML12 cells were cultured in a 1:1 mixture of DMEM and Ham's F12 medium (DMEM/F12 medium) (Life Technologies) containing 1× insulin-transferrin-selenium (Life Technologies), 40 ng/ml dexamethasone, and 10% FBS (Life Technologies). HepG2 cells were maintained in DMEM/F12 medium supplemented with 10% FBS and insulin (Sigma). HEK293 cells were cultured in DMEM supplemented with 10% FBS. To examine the effect of Zhx2 on endogenous Mup expression, 2.5 μg of Zhx2-GFP or pcDNA3.1 empty vector control (E.V.) were transfected into 10^6 AML12 cells using the Neon Transfection System (Life Technologies) and then seeded onto two wells of a 6-well plate. After 48 h, when cells were near confluent, Zhx2-GFP expression was visualized using fluorescence microscopy to ensure robust expression. Cells were harvested in RNAzol reagent and frozen at −80 °C until RNA was prepared. All transfections were done in duplicate and repeated three times. To test the effect of Zhx2 on Mup20 promotor activity, HepG2 or AML12 cells were seeded at 10^5/well in 24-well cell culture plates. The following day, 750 ng of expression plasmid (Zhx2 or E.V.) was co-transfected with 250 ng of luciferase reporter plasmid (pGL4 or Mup20^{P}-Luc) and 10 ng of *Renilla* luciferase vector (pRL, Promega) into cells using Lipofectamine 2000 (Life Technologies) or TurboFect (Thermo Fisher Scientific) according to the instructions of the manufacturer. To test the effect of Gal4DBD-Zhx2 on Mup20^{P}-luc and SV40^{P}-luc with or without UAS elements, HEK293 cells were seeded at 2×10^5/well in 24-well cell culture plates and transfected as described above. Cell lysates were prepared after 48 h using the passive lysis buffer (Promega). The firefly/*Renilla* luciferase levels were determined in duplicate using the Dual-Luciferase reporter assay system (Promega). All transfections were done in duplicate and repeated three times.

RT quantitative real-time PCR

RNA was prepared from frozen tissues (~100 mg) or AML12 cells using RNAzol RT reagent (Molecular Research Center) according to the instructions of the manufacturer. One microgram of RNA was reverse-transcribed to cDNA using the iScript^{TM} cDNA synthesis kit (Bio-Rad). qPCR reactions were prepared with SsoAdvanced Universal SYBR Green Supermix (Bio-Rad) and amplified in a Bio-Rad CFX96 real-time PCR system. Oligonucleotides were obtained from Integrated DNA Technologies (Coralville, IA), and their sequences are shown in supplemental Table 2. The qPCR Ct values were normalized to ribosomal protein L30 levels and reported as normalized expression of the indicated gene using the ΔCt method (43). L30 was used because we found that L30 mRNA levels remain stable across different developmental time points (44). In all cases, primers spanned introns so that amplicons from cDNA and any contaminating genomic DNA would be of different lengths and readily detected by melting curve analysis of completed PCR reactions.

Analysis of Mup protein levels in mouse liver and urine

Mup protein levels in liver and urine from $Zhx2^{fl}$, $Zhx2^{\Delta hep}$ or $Zhx2^{KO}$ mice were analyzed by Western blotting. Liver protein lysates were prepared in radioimmune precipitation assay

buffer, and protein concentrations of lysates were determined using a Bradford protein assay reagent (Bio-Rad). Urine was also collected from adult male $Zhx2^{fl}$, $Zhx2^{\Delta hep}$ or $Zhx2^{KO}$ mice and clarified by centrifugation at 6700 × *g* for 4 min. Total liver protein or urine for each sample was resolved by electrophoresis using 15% SDS-PAGE and transferred to PVDF membranes. After blocking with 5% dry milk, analysis of Mup proteins was performed using a goat anti-mouse Mup polyclonal antiserum (Cedarlane Laboratories, catalog no. GAM/MUP) and an enhanced chemiluminescence kit (Pierce). For whole urinary protein analysis, urinary proteins were separated by 15% SDS-PAGE and stained by LabSafe Gel Blue reagent (G-Biosciences, St. Louis, MO).

ChIP

Chromatin preparation was performed as described previously (45, 46) with minor changes. Mouse livers were harvested, minced, cross-linked in 1.42% formaldehyde for 15 min followed by quenching with a 1/10 volume of 1.25 M glycine solution for 5 min and washed twice with 1× PBS containing proteinase inhibitors. Nuclear extracts were prepared by Dounce homogenization in cell lysis buffer (5 mM PIPES (pH 8), 85 mM KCl, 0.5% Igepal, and proteinase inhibitors) followed by centrifugation. Chromatin fragmentation was performed by sonication (Fisher Scientific sonic dismembrator, model 500) in nucleus lysis buffer (50 mM Tris-HCl (pH 8), 10 mM EDTA, 0.5%SDS, and proteinase inhibitors). ChIP was performed using antibodies (rabbit anti-Zhx2, made for us by Bethyl Labs) and rabbit IgG with the Magna ChIP HiSens kit (Millipore) following the instructions of the manufacturer. ChIP DNA samples were analyzed by quantitative PCR using SsoAdvancedTM Universal SYBR Green Supermix (Bio-Rad) and a Bio-Rad CFX96 real-time PCR system. Primers used for ChIP are shown in supplemental Table 2.

Statistical analysis

All values within a group were averaged and plotted as mean ± S.D. *p* values were calculated between two groups using Student's *t* test. $p \leq 0.05$ was considered significant. Data were graphed and analyzed using GraphPad Prism 6 software.

Author contributions—J. J. conducted the majority of the experiments, analyzed data, and wrote the first draft of the paper. K. T. C., and J. P. conducted additional experiments. M. L. P. provided ideas, evaluated data, and edited the manuscript. B. T. S. provided the initial idea for the experiments, supervised the experimental work, and wrote the final manuscript.

Acknowledgments—Floxed Zhx2 mice were obtained from the trans-NIH Knock-Out Mouse Project. TTR-Zhx2 transgenic mice were generated at the University of Kentucky Transgenic Mouse Core Facility. We thank Changcheng Zhou (University of Kentucky) for pCMX-Gal4 and Doug Harrison (University of Kentucky) for pUAST. We also thank Alexandra Nail for helpful comments on the manuscript.

References

1. Finlayson, J. S., Asofsky, R., Potter, M., and Runner, C. C. (1965) Major urinary protein complex of normal mice: origin. *Science* **149,** 981–982
2. Ganfornina, M. D., Gutiérrez, G., Bastiani, M., and Sánchez, D. (2000) A phylogenetic analysis of the lipocalin protein family. *Mol. Biol. Evol.* **17,** 114–126
3. Gómez-Baena, G., Armstrong, S. D., Phelan, M. M., Hurst, J. L., and Beynon, R. J. (2014) The major urinary protein system in the rat. *Biochem. Soc. Trans.* **42,** 886–892
4. Beynon, R. J., and Hurst, J. L. (2003) Multiple roles of major urinary proteins in the house mouse, *Mus domesticus*. *Biochem. Soc. Trans.* **31,** 142–146
5. Chamero, P., Marton, T. F., Logan, D. W., Flanagan, K., Cruz, J. R., Saghatelian, A., Cravatt, B. F., and Stowers, L. (2007) Identification of protein pheromones that promote aggressive behaviour. *Nature* **450,** 899–902
6. Kaur, A. W., Ackels, T., Kuo, T. H., Cichy, A., Dey, S., Hays, C., Kateri, M., Logan, D. W., Marton, T. F., Spehr, M., and Stowers, L. (2014) Murine pheromone proteins constitute a context-dependent combinatorial code governing multiple social behaviors. *Cell* **157,** 676–688
7. Bishop, J. O., Clark, A. J., Clissold, P. M., Hainey, S., and Francke, U. (1982) Two main groups of mouse major urinary protein genes, both largely located on chromosome 4. *EMBO J.* **1,** 615–620
8. Hastie, N. D., Held, W. A., and Toole, J. J. (1979) Multiple genes coding for the androgen-regulated major urinary proteins of the mouse. *Cell* **17,** 449–457
9. Logan, D. W., Marton, T. F., and Stowers, L. (2008) Species specificity in major urinary proteins by parallel evolution. *PLoS ONE* **3,** e3280
10. Shaw, P. H., Held, W. A., and Hastie, N. D. (1983) The gene family for major urinary proteins: expression in several secretory tissues of the mouse. *Cell* **32,** 755–761
11. Knopf, J. L., Gallagher, J. F., and Held, W. A. (1983) Differential, multihormonal regulation of the mouse major urinary protein gene family in the liver. *Mol. Cell Biol.* **3,** 2232–2240
12. Szoka, P. R., and Paigen, K. (1978) Regulation of mouse major urinary protein production by the Mup-A gene. *Genetics* **90,** 597–612
13. Kawata, H., Yamada, K., Shou, Z., Mizutani, T., and Miyamoto, K. (2003) The mouse zinc-fingers and homeoboxes (ZHX) family: ZHX2 forms a heterodimer with ZHX3. *Gene* **323,** 133–140
14. Kawata, H., Yamada, K., Shou, Z., Mizutani, T., Yazawa, T., Yoshino, M., Sekiguchi, T., Kajitani, T., and Miyamoto, K. (2003) Zinc-fingers and homeoboxes (ZHX) 2, a novel member of the ZHX family, functions as a transcriptional repressor. *Biochem. J.* **373,** 747–757
15. Yamada, K., Kawata, H., Shou, Z., Hirano, S., Mizutani, T., Yazawa, T., Sekiguchi, T., Yoshino, M., Kajitani, T., and Miyamoto, K. (2003) Analysis of zinc-fingers and homeoboxes (ZHX)-1-interacting proteins: molecular cloning and characterization of a member of the ZHX family, ZHX3. *Biochem. J.* **373,** 167–178
16. Spear, B. T., Jin, L., Ramasamy, S., and Dobierzewska, A. (2006) Transcriptional control in the mammalian liver: liver development, perinatal repression, and zonal gene regulation. *Cell Mol. Life Sci.* **63,** 2922–2938
17. Abelev, G. I., Perova, S. D., Khramkova, Z. A., Postnikova, A., and Irlin, I. S. (1963) Production of embryonal alphaglobulin by transplantable mouse hepatomas. *Transplantation* **1,** 174–180
18. Belayew, A., and Tilghman, S. M. (1982) Genetic analysis of α-fetoprotein synthesis in mice. *Mol. Cell Biol.* **2,** 1427–1435
19. Olsson, M., Lindahl, G., and Ruoslahti, E. (1977) Genetic control of α-fetoprotein synthesis in the mouse. *J. Exp. Med.* **145,** 819–827
20. Perincheri, S., Dingle, R. W., Peterson, M. L., and Spear, B. T. (2005) Hereditary persistence of α-fetoprotein and H19 expression in liver of BALB/cJ mice is due to a retrovirus insertion in the Zhx2 gene. *Proc. Natl. Acad. Sci., U.S.A.* **102,** 396–401
21. Perincheri, S., Peyton, D. K., Glenn, M., Peterson, M. L., and Spear, B. T. (2008) Characterization of the ETnII-α endogenous retroviral element in the BALB/cJ Zhx2 (Afr1) allele. *Mamm. Genome* **19,** 26–31
22. Blankenhorn, E. P., Duncan, R., Huppi, K., and Potter, M. (1988) Chromosomal location of the regulator of mouse α-fetoprotein, afr-1. *Genetics* **119,** 687–691
23. Peyton, D. K., Huang, M.-C., Giglia, M. A., Hughes, N. K., and Spear, B. T. (2000) The α-fetoprotein promoter is the target of Afr1-mediated postnatal repression. *Genomics* **63,** 173–180

24. Morford, L. A., Davis, C., Jin, L., Dobierzewska, A., Peterson, M. L., and Spear, B. T. (2007) The oncofetal gene glypican 3 is regulated in the postnatal liver by zinc fingers and homeoboxes 2 and in the regenerating liver by α-fetoprotein regulator 2. *Hepatology* **46,** 1541–1547
25. Pachnis, V., Belayew, A., and Tilghman, S. M. (1984) Locus unlinked to α-fetoprotein under the control of the murine *raf* and *Rif* genes. *Proc. Natl. Acad. Sci. U.S.A.* **81,** 5523–5527
26. Gargalovic, P. S., Erbilgin, A., Kohannim, O., Pagnon, J., Wang, X., Castellani, L., Leboeuf, R., Peterson, M. L., Spear, B. T., and Lusis, A. J. (2010) Quantitative trait locus mapping and identification of zhx2 as a novel regulator of plasma lipid metabolism. *Circ. Cardiovasc. Genet.* **3,** 60–67
27. Shen, H., Luan, F., Liu, H., Gao, L., Liang, X., Zhang, L., Sun, W., and Ma, C. (2008) ZHX2 is a repressor of α-fetoprotein expression in human hepatoma cell lines. *J Cell Mol. Med.* **12,** 2772–2780
28. Yue, X., Zhang, Z., Liang, X., Gao, L., Zhang, X., Zhao, D., Liu, X., Ma, H., Guo, M., Spear, B. T., Gong, Y., and Ma, C. (2012) Zinc fingers and homeoboxes 2 inhibits hepatocellular carcinoma cell proliferation and represses expression of Cyclins A and E. *Gastroenterology* **142,** 1559–1570.e2
29. Cheetham, S. A., Smith, A. L., Armstrong, S. D., Beynon, R. J., and Hurst, J. L. (2009) Limited variation in the major urinary proteins of laboratory mice. *Physiol. Behav.* **96,** 253–261
30. Duncan, R., Matthai, R., Huppi, K., Roderick, T., and Potter, M. (1988) Genes that modify expression of major urinary proteins in mice. *Mol. Cell Biol.* **8,** 2705–2712
31. Creasy, K. T., Jiang, J., Ren, H., Peterson, M. L., and Spear, B. T. (2016) Zinc fingers and homeoboxes 2 (Zhx2) regulates sexually dimorphic *Cyp* gene expression in the adult mouse liver. *Gene Exp.* **17,** 7–17
32. Kwak, J., Grigsby, C. C., Rizki, M. M., Preti, G., Köksal, M., Josue, J., Yamazaki, K., and Beauchamp, G. K. (2012) Differential binding between volatile ligands and major urinary proteins due to genetic variation in mice. *Physiol. Behav.* **107,** 112–120
33. Holloway, M. G., Laz, E. V., and Waxman, D. J. (2006) Codependence of growth hormone-responsive, sexually dimorphic hepatic gene expression on signal transducer and activator of transcription 5b and hepatic nuclear factor 4α. *Mol. Endocrinol.* **20,** 647–660
34. Dragani, T. A., Manenti, G., Sacchi, M. R., Colombo, B. M., and Della Porta, G. (1989) Major urinary protein as a negative tumor marker in mouse hepatocarcinogenesis. *Mol. Carcinog.* **2,** 355–360
35. Ciaranello, R. D., Hoffman, H. J., Shire, J. G., and Axelrod, J. (1974) Genetic regulation of the catecholamine biosynthetic enzymes: II: inheritance of tyrosine hydroxylase, dopamine-β-hydroxylase, and phenylethanolamine *N*-methyltransferase. *J. Biol. Chem.* **249,** 4528–4536
36. Ciaranello, R. D., Lipsky, A., and Axelrod, J. (1974) Association between fighting behavior and catecholamine biosynthetic enzyme activity in two inbred mouse sublines. *Proc. Natl. Acad. Sci. U.S.A.* **71,** 3006–3008
37. Dow, H. C., Kreibich, A. S., Kaercher, K. A., Sankoorikal, G. M., Pauley, E. D., Lohoff, F. W., Ferraro, T. N., Li, H., and Brodkin, E. S. (2011) Genetic dissection of intermale aggressive behavior in BALB/cJ and A/J mice. *Genes Brain Behav.* **10,** 57–68
38. Bis, J. C., Kavousi, M., Franceschini, N., Isaacs, A., Abecasis, G. R., Schminke, U., Post, W. S., Smith, A. V., Cupples, L. A., Markus, H. S., Schmidt, R., Huffman, J. E., Lehtimäki, T., Baumert, J., Münzel, T., *et al.* (2011) Meta-analysis of genome-wide association studies from the CHARGE consortium identifies common variants associated with carotid intima media thickness and plaque. *Nat. Genet.* **43,** 940–947
39. Li, C., Chen, W., Jiang, F., Simino, J., Srinivasan, S. R., Berenson, G. S., and Mei, H. (2015) Genetic association and gene-smoking interaction study of carotid intima-media thickness at five GWAS-indicated genes: the Bogalusa Heart Study. *Gene* **562,** 226–231
40. Zhou, Y., Jiang, L., and Rui, L. (2009) Identification of MUP1 as a regulator for glucose and lipid metabolism in mice. *J. Biol. Chem.* **284,** 11152–11159
41. Yan, C., Costa, R. H., Darnell, J. E., Jr., Chen, J. D., and Van Dyke, T. A. (1990) Distinct positive and negative elements control the limited hepatocyte and choriod plexus expression of transthyretin in transgenic mice. *EMBO J.* **9,** 869–878
42. Brand, A. H., and Perrimon, N. (1993) Targeted gene expression as a means of altering cell fates and generating dominant phenotypes. *Development* **118,** 401–415
43. Livak, K. J., and Schmittgen, T. D. (2001) Analysis of relative gene expression data using real-time quantitative PCR and the $2(-\Delta\Delta$ C(T)) method. *Methods* **25,** 402–408
44. Waxman, S., and Wurmbach, E. (2007) De-regulation of common housekeeping genes in hepatocellular carcinoma. *BMC Genomics* **8,** 243
45. Nelson, J. D., Denisenko, O., and Bomsztyk, K. (2006) Protocol for the fast chromatin immunoprecipitation (ChIP) method. *Nat. Protoc.* **1,** 179–185
46. O'Geen, H., Echipare, L., and Farnham, P. J. (2011) Using ChIP-seq technology to generate high-resolution profiles of histone modifications. *Methods Mol. Biol.* **791,** 265–286